Relevance of Oxocyclam from Palladium(II) Coordination to Radiopharmaceutical Development

Maher Hojorat, Julie Pineau, Cathryn Driver, David Esteban-Gómez, Marie Cordier, Jan Rijn Zeevaart, Carlos Platas-Iglesias, Luís Lima, Nathalie Le Bris, Raphaël Tripier

Relevance of Oxocyclam from Palladium(II) Coordination to Radiopharmaceutical Development

Maher Hojorat,[a],‡ Julie Pineau,[a],‡ Cathryn H. S. Driver,[b] David Esteban-Gómez,[c] Marie Cordier,[d] Jan Rijn Zeevaart,[b] Carlos Platas-Iglesias,[c] Luís M. P. Lima,[e] Nathalie Le Bris,[a],* and Raphaël Tripier[a],*

[a] Univ Brest, UMR CNRS 6521 CEMCA, 6 avenue Victor le Gorgeu, 29238 Brest, France.
[b] South African Nuclear Energy Corporation, Radiochemistry and PreClinical Imaging Facility, Elias Motsoaledi Street, R104 Pelindaba, North West, 0240, South Africa.
[c] Departamento de Química, Facultade de Ciencias & Centro Interdisciplinar de Química e Bioloxía (CICA), Universidade da Coruña, 15071 A Coruña, Spain.
[d] Univ Rennes, CNRS, ISCR (Institut des Sciences Chimiques de Rennes) UMR 6226, 35000 Rennes, France.
[e] Instituto de Tecnologia Química e Biológica António Xavier, Universidade Nova de Lisboa, Av. da República, 2780–157 Oeiras, Portugal.

KEYWORDS. oxocyclam • bifunctional oxocyclam • complexation • palladium(II) • palladium-109 • radiolabeling

ABSTRACT: We provide a comprehensive study of the coordination of **oxocyclam** with palladium(II), presenting a novel bifunctional analogue, ***p*-H$_2$N-Bn-oxocyclam,** bearing an aniline pendant. The complexation of palladium(II) with **oxocyclam** was examined by various techniques, including NMR analysis and potentiometric titrations which revealed that the Pd(II) complex can adopt different configurations such as *trans*-I and *trans*-III. In addition, **oxocyclam** forms a thermodynamically stable palladium(II) complex, the stabilization being attributed to the deprotonation of the amide function. The crystal structures of [Pd(H$_{-1}$**oxocyclam**)]$^+$ and [Pd(**oxocyclam**)]$^{2+}$ were obtained, revealing the structural details previously anticipated, including, in the second case, the presence of the proton on the carbonyl oxygen atom. Additionally, the study explored the redox behavior of the Pd(II)-**oxocyclam** complex through reduction and oxidation voltammograms at different pH values. Successful ^{109}Pd-labeling of **oxocyclam** and ***p*-H$_2$N-Bn-oxocyclam** at pH 3.5 demonstrated high labeling efficiencies, whatever the species formed. The stability of the radiocomplexes was assessed and moderate transchelation towards EDTA was observed. Overall, **oxocyclam** displayed favorable properties for Pd(II) coordination and radiolabeling, suggesting its potential as a chelating agent for this metal in palladium-based applications.

INTRODUCTION

Palladium(II) has been acknowledged as a noteworthy cation in the medical field since the 1960s when its antitumor properties, similar to those of platinum(II), were explored.[1–3] In 1979, Graham and Williams reported the antiviral, antifungal, and antimicrobial properties of palladium(II) complexes.[4] More recently, various palladium(II)-based drugs or therapeutic agents have been employed in more sophisticated techniques, such as targeted photodynamic therapy for localized cancer treatment.[5]

In the field of nuclear medicine, palladium radioisotopes were first used in the early 1970s. Molecules based on palladium-109 (^{109}Pd) were described for controlling homograft rejection[6,7] and in 1987, palladium-103 (^{103}Pd) was introduced as implanted seeds for brachytherapy.[8,9] Despite these initial applications, subsequent developments have remained very limited. Nonetheless, these radionuclides are likely to receive increasing attention in therapy due to their beneficial radiophysical characteristics, given the increasing demand for radiopharmaceuticals for cancer treatment and personalized medicine. ^{103}Pd- and ^{109}Pd-nuclides have half-lives ($t_{1/2}$) of 17 days and 13.7 hours, respectively. ^{103}Pd-nuclide decays by electron capture (EC) along with Auger electron emissions, and ^{109}Pd-nuclide decays by β^- particle emission, leading to stable daughter nuclides ^{103}Rh and ^{111}Ag, respectively.[10,11]

The optimal use of therapeutic radiopharmaceuticals is achieved in combination with a radiodiagnostic agent, which allows for disease staging and treatment monitoring.[12] Diagnostic radiotracers employ radionuclides, often of metallic elements, emitting positrons (β^+) and photons (γ) for PET and SPECT imaging, respectively.[13] For the development of radiopharmaceuticals using metallic radionuclides, the radiometals produced in their cationic form must be complexed with a chelator that meets the requirements for *in vivo* applications.[14,15] The radiochelate formed upon complexation should exhibit high stability, both thermodynamically and kinetically, and must be bifunctional. *C*-functionalization of the chelator backbone has often proved to be the most efficient strategy towards

BCAs (Bifunctional Chelating Agents), as it avoids the sacrifice of the metal-coordinating heteroatom functionalities.[16–20]

Despite the interesting properties of palladium radioisotopes, they have been little used in the development of radiopharmaceuticals. The limited number of studies reported concerns the use of a few ligands, such as DTPA[21] and porphyrins [6,7,22,23]. The primary reason for this is that the palladium coordination chemistry does not align with the chelators considered as gold standards in nuclear medicine, namely the DOTA and NOTA derivatives. Palladium(II) primarily forms four-coordinated complexes with a square-planar geometry, being incompatible with these ligands.[24] Although numerous ligands have been proposed for Pd(II) complexation[25] and some works have demonstrated high thermodynamic stability for certain complexes, kinetic inertness studies are very rare.[26,27] Our recent review showed that macrocyclic polyamines, such as the well-known **cyclam** scaffold**,** are advantageous for coordinating Pd(II).[28] C**yclam** (Figure 1) forms highly stable and inert complexes with small transition metal ions, including Pd(II) for which, an extremely high stability constant ($\log K_{PdL} = 56.9$) was estimated.[29] More recently, we reported a comprehensive study highlighting picolinate-cyclam **TE1PA** as a highly relevant chelator for natural palladium and subsequently for palladium-109.[30] The structural, thermodynamic, kinetic and radiolabeling studies of **TE1PA** with palladium(II), as well as the comparison of this complex with structurally related derivatives, supported further development of Pd(II)-**TE1PA** derivatives as leading candidates for targeted nuclear medicine.

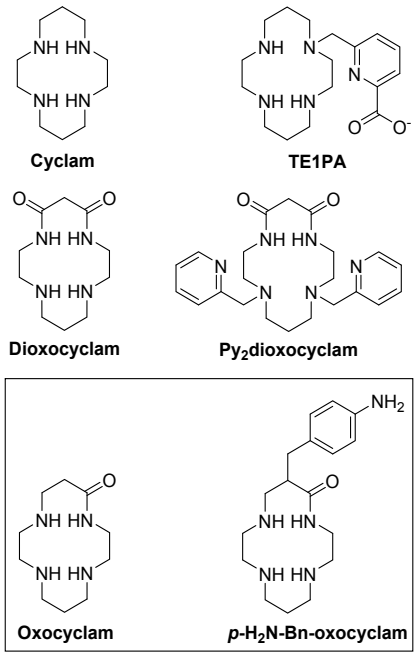

Figure 1. Cyclam-based ligands discussed in this article.

In order to further obtain new information on palladium(II) coordination chemistry relevant for the development of new radiopharmaceuticals, our attention was turned to **oxocyclam** derivatives (Figure 1). **Dioxocyclam** is an interesting chelator featuring two amide functions and two secondary amines. When interacting with divalent transition metals such as Pt(II) or Cu(II), **dioxocyclam** derivatives are recognized for their capacity to act as tetradentate ligands, leading to the formation of doubly deprotonated complexes.[31,32] Kimura and coworkers have previously documented Pd(II) complexes of a **dioxocyclam** *N,N'*-dialkylated with 2-pyridylmethyl arms, known as **Py$_2$dioxocyclam**.[33] Two Pd(II)-complexes formed with this ligand were isolated in the solid state from aqueous solutions at different pH values. The crystal structure of the [Pd(**Py$_2$dioxocyclam**)]$^{2+}$ complex, obtained at pH = 6, revealed a square-planar geometry with Pd(II) coordinated by two tertiary amines and two pyridyl nitrogen atoms. However, crystallization at pH = 10 afforded the doubly deprotonated species [Pd(H$_{-2}$**Py$_2$dioxocyclam**)], which exhibits a similar square-planar geometry with Pd(II) four-coordinated by the two deprotonated nitrogen atoms of the amide functions and the two tertiary amines. The reversible interconversion between these complexes in solution is facilitated by pH-dependent deprotonation of the amide groups.

Upon a more in-depth literature survey, we noticed that "simple" **oxocyclam** has never been studied as a Pd(II) chelator (Figure 1). Thus, we have decided to investigate this ligand in order to understand the real influence of the macrocyclic amide function on palladium(II) coordination under specific conditions. Ligand protonation constants and stability constants of the copper(II) and nickel(II) complexes were reported previously. In the pH range 2.5–7.0, copper(II) formed two complexes, [CuL]$^{2+}$ and [Cu(H$_{-1}$L)]$^{+}$, while nickel(II) formed exclusively the deprotonated complex [Ni(H$_{-1}$L)]$^{+}$.[34] In 1992, **oxocyclam** was also investigated by Riche *et al*. in the context of nuclear medicine for SPECT application with technetium-99m.[35] This study highlighted the remarkable kinetic and thermodynamic stability of the [^{99m}TcO$_2$-**oxocyclam**] complex and represented one of the rare examples of the use of **oxocyclam** derivatives for nuclear medicine applications. Following these observations, it was then assumed that **oxocyclam** should also exhibit interesting behavior for the complexation of Pd(II), including Pd-radionuclides.

Herein, we report a comprehensive study of the coordination of **oxocyclam** with Pd(II) by means of NMR, UV-vis spectroscopy, solid state chemistry, potentiometry and electrochemistry. Particular attention was given to the form of the amide function (in relation with its protonation or evolution to other forms) and its influence on the metal cation coordination. DFT calculations were also performed to support the experimental study. Furthermore, an oxocyclam BCA, ***p*-H$_2$N-Bn-oxocyclam**, was designed and synthesized by a *C*-functionalization strategy, taking advantage of one of our previously described procedures.[36,37] This compound is suitable for conjugation with targeting moieties for vectorized radio-immunotherapy applications after activation of the aniline function. Both **oxocyclam** and ***p*-H$_2$N-Bn-oxocyclam** ligands were labeled with ^{109}Pd-nuclide and the stability of the radiocomplexes was studied in different media, which

confirmed the promising results obtained with the cold metal.

RESULTS AND DISCUSSION

Ligand synthesis. The synthesis of **oxocyclam** (5-oxo-1,4,8,11-tetraazacyclotetradecane) was reported by Hay *et al*. in 1985 by reacting methyl acrylate with the linear tetraamine *N,N'*-bis(*2*-aminoethyl)-*1,3*-propanediamine.[34] The commercially available **oxocyclam** was used as such for this work [see experimental section - material]. The new oxocyclam BCA, ***p*-H_2N-Bn-oxocyclam,** was synthesized according to the synthetic pathway presented in Figure 2. Compounds **1-4** were obtained following a procedure described previously by our group.[36–38] A catalytic hydrogenolysis of compound **4** carried out at room temperature easily led to the debenzylated analogue ***p*-H_2N-Bn-oxocyclam** in 87% yield. This molecule is a key intermediate for obtaining different BCAs, for instance the isothiocyanate derivative, by reaction with thiophosgene using a standard procedure.[37] The structure of ***p*-H_2N-Bn-oxocyclam** was confirmed by NMR and FT-IR spectroscopy, in addition to HRMS analysis (see SI, Figures S1-S4).

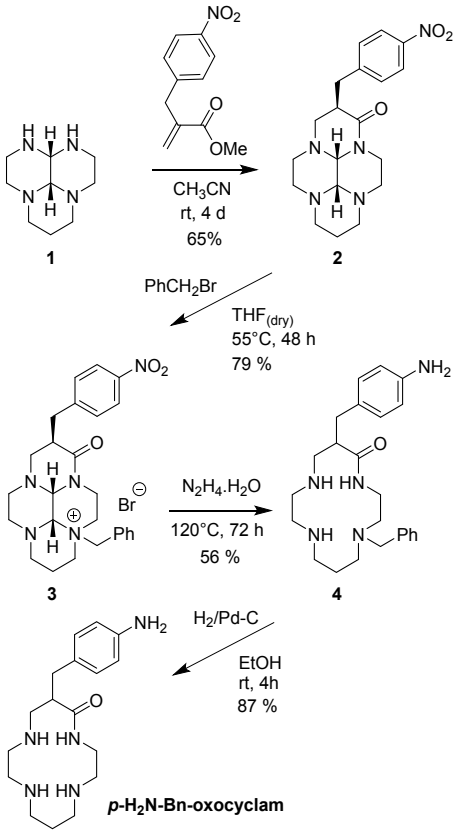

Figure 2. Synthesis of the bifunctional chelating agent ***p*-H_2N-Bn-oxocyclam**.

Acid-base properties. We first investigated the acid-base properties of **oxocyclam** by means of potentiometric measurements. The protonation constants obtained are comparable to those previously reported in the literature ($\log K_1 = 9.40$, $\log K_2 = 6.65$ and $\log K_3 = 2.87$), although slightly higher due to the variation in experimental conditions under which they were determined (Table 1).[34] The increase in log K_{HiL} values is most likely a consequence of the much higher ionic strength adopted in our determinations (1.0 M in KCl *vs* 0.2 M in $NaClO_4$) as well as the likely formation of a weak Na(I) complex in the literature conditions. As expected, three protonation constants were found for the three secondary amine functions of **oxocyclam** with $\log K_1 = 10.89$, $\log K_2 = 7.42$ and $\log K_3 = 3.61$, while the deprotonation of the amide N-H is not attainable under these conditions. The speciation diagram for **oxocyclam** as a function of pH can then be plotted, taking these protonation constants into account (see in SI, Figure S5).

The protonation study and palladium(II) complexation experiments on the bifunctional analogue ***p*-H_2N-Bn-oxocyclam** were not performed, given our previous studies showing that the added *C*-appended group does not drastically affect the properties of the ligand.[20]

Table 1. Overall (log β_{MHiL}) and stepwise (log K_{MHiL}) equilibrium constants for oxocyclam (= L) as determined by potentiometry at 25 °C in 1.0 M KCl aqueous solution.

Equilibrium reaction [a]	log β_{MHiL}
$L + H^+ \rightleftarrows HL$	10.89(1)
$L + 2H^+ \rightleftarrows H_2L$	18.31(1)
$L + 3H^+ \rightleftarrows H_3L$	21.92(1)
$Pd^{2+} + L \rightleftarrows PdL$	28.58(1)
$Pd^{2+} + L + H^+ \rightleftarrows PdHL$	31.53(1)
$Pd^{2+} + L \rightleftarrows PdH_{-1}L + H^+$	25.44(1)
	log K_{MHiL}
$L + H^+ \rightleftarrows HL$	10.89
$HL + H^+ \rightleftarrows H_2L$	7.42
$H_2L + H^+ \rightleftarrows H_3L$	3.61
$Pd^{2+} + L \rightleftarrows PdL$	28.58
$PdL + H^+ \rightleftarrows PdHL$	2.95
$PdH_{-1}L + H^+ \rightleftarrows PdL$	3.14

[a] Charges are omitted for clarity.

Complexation studies. The palladium(II) complexation by **oxocyclam** (Table 1) could be fully studied by direct potentiometric titrations. This methodology was firstly envisioned to measure the thermodynamic constants and secondly to identify the different species present in solution depending on the pH. Unlike what was found for the series of tetraazamacrocyclic ligands including **TE1PA**,[30] there was no need to resort to UV spectrophotometric experiments to attain these measurements. Indeed, despite the relatively slow kinetics of palladium(II) complexation in the acidic pH range, we found that complexation takes place from the most acidic pH up until pH=4, which therefore allows full advantage to be taken of the potentiometric technique.

The formation constant determined for the palladium(II) **oxocyclam** complex ($\log K_{PdL} = 28.58$) is much lower than that found for the palladium(II) complex of **cyclam** ($\log K_{PdL} = 56.9$)[29] and some other *N*-monosubstituted cyclams ($\log K_{PdL} \geq 38.4$)[30] but it is much higher than for the *N*-tetra(2-hydroxyethyl) cyclam with $\log K_{PdL} = 18.32$.[39] In addition to the $[Pd(\mathbf{oxocyclam})]^{2+}$ species (PdL), **oxocyclam** also forms a mono-protonated species $[Pd(H\mathbf{oxocyclam})]^{3+}$ (PdHL) at low pH, as well as a mono

deprotonated species [Pd(H$_{-1}$**oxocyclam**)]$^{+}$ (PdH$_{-1}$L). This latter species should undoubtedly correspond to the deprotonation of the amide function of the ligand (pK_a = 3.14), which was also reported to occur for the copper(II) complex at slightly higher pH (pK_a = 5.54).[34] From the determined equilibrium constants, it is possible to plot a speciation diagram at varying pH for the **oxocyclam** palladium(II) complex (Figure 3). This plot evidences that the fully deprotonated complex (including the deprotonated amide) is the sole species around neutral pH, while two additional species exist between *ca.* pH 2–5. At lower pH, a competition taking place between the **oxocyclam** complex species and the palladium(II) chloride species (essentially $PdCl_3$ and $PdCl_4$) is visible, which assists in the determination of the palladium(II) complexation by potentiometry. Overall, we may conclude that **oxocyclam** forms a thermodynamically stable palladium(II) complex which is stabilized by the deprotonation of the amide function.

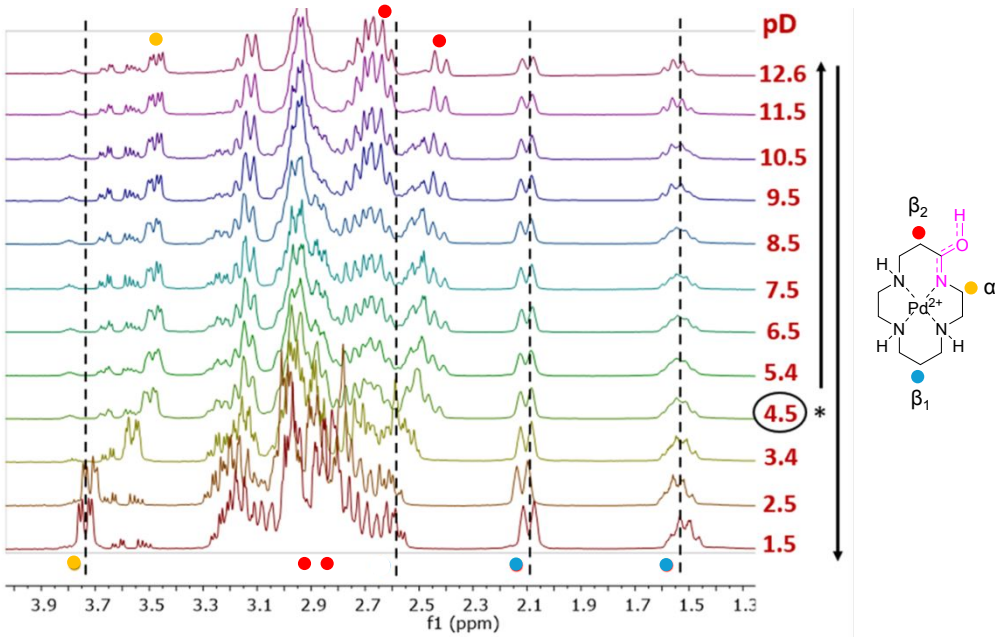

Figure 4. ^{1}H NMR (400 MHz, D_2O, 25 °C) spectra of Pd(II)-**oxocyclam** (ratio 1:1) at different pD. The asterisk indicates the pD above which the [Pd(H$_{-1}$**oxocyclam**)]$^{+}$ species is largely predominant. Arrows show sense of variation of the pD during the experiment. Peaks belonging to the β_1, β_2, and α protons to the amide are indicated by the blue, red and yellow dots, respectively.

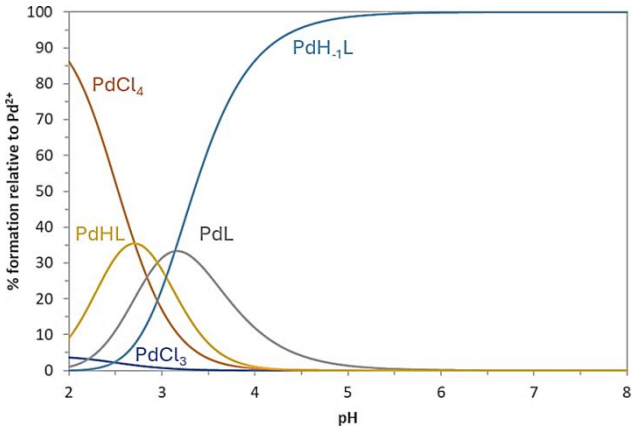

Figure 3. Species distribution diagram of Pd(II) in presence of **oxocyclam** as determined by potentiometry at 25 °C in 1.0 M KCl aqueous solution and calculated at $[Pd^{2+}]_{tot}$ = $[L]_{tot}$ = 1×10^{-3} M (**oxocyclam** = L). Charges are omitted for clarity.

Considering the potentiometric studies, the acid-base properties of Pd(II)-**oxocyclam** complex were studied by NMR in D_2O at different pD values. The complexation was performed at room temperature for 60 minutes at pD 4.5

(since at more acidic values a precipitate was observed) in the presence of stoichiometric amounts of Pd(II) and **oxocyclam.** The pD was adjusted with a deuterated sodium hydroxide or deuterium chloride solution before recording each spectrum at 25 °C. ^{1}H NMR spectra are reported in Figure 4, while ^{13}C NMR spectra and 2D NMR experiments (^{1}H-^{1}H COSY, ^{1}H-^{13}C HSQC and ^{1}H-^{13}C HMBC NMR spectra) are included in SI (Figures S6-S15) at the representative pD values of 1.4, 7.6, and 12.7 (adjusted pH values of 1.0, 7.2 and 12.3, respectively).

In the aim to identify possible metallic species present in solution, the complexation was monitored by NMR analysis upon incremental addition of Na_2PdCl_4 to a solution of the ligand in deuterium oxide until 1 equivalent was reached, at a constant pD = 4.5 (pH = 4.1)[40] where [Pd(H$_{-1}$**oxocyclam**)]$^{+}$ (PdH$_{-1}$L) is predominant. For each experiment, the solution was heated at 80 °C for 30 minutes to reach thermodynamic equilibrium. The solution was then returned to room temperature and the pD was readjusted to 4.5 before recording the ^{1}H NMR spectra at two different temperatures

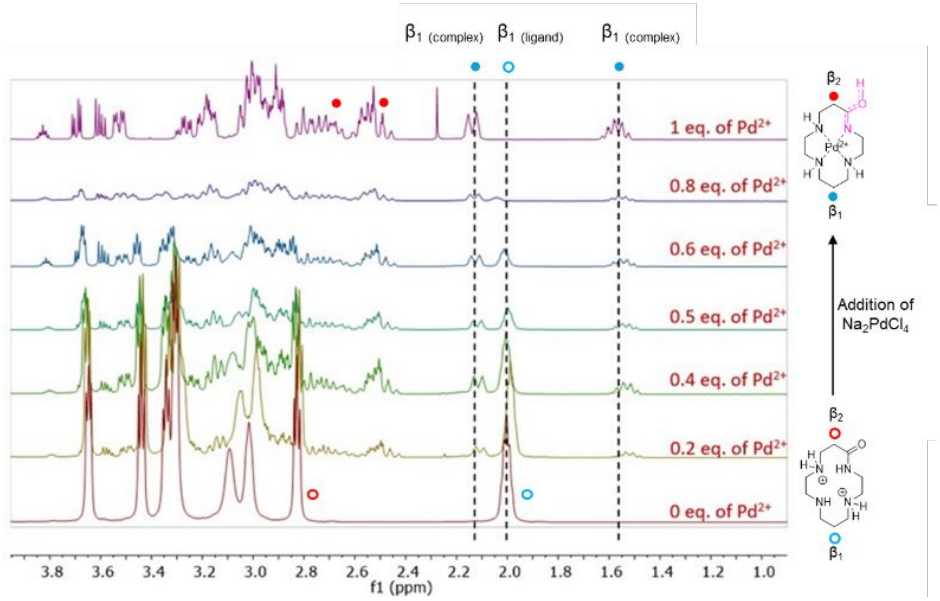

Figure 5. ^{1}H NMR spectra (400 MHz, D_2O, 25 °C) of **oxocyclam** with increasing amounts of Pd(II) salt (Na_2PdCl_4) at pD = 4.5 (pH = 4.1).

The ^{1}H NMR spectra are rather complicated, but the analysis of the peaks belonging to the β_1, β_2, and α protons to the amide (Figure 4) provides useful insights into the behavior of the Pd(II)-**oxocyclam** complex at different pD values. The peaks observed around 1.5 and 2.1 ppm were assigned to the β_1 hydrogen atoms signals as confirmed by the HSQC ^{1}H-^{13}C NMR spectrum (see in SI, Figure S8, S11 and S14), where cross-peaks correlate these two peaks with the β1 carbon atom. There was no significant change in the chemical shifts of the β_1 protons by varying the pD of the solution. In contrast, the signals due to the β_2 and α protons experience remarkable changes in their chemical shift, shifting upfield as the pD is raised from 3.4 to 5.4. The β_2 protons of the complex at the different pDs are not clearly identified on the ^{1}H NMR spectra but appear around 2.9 ppm in very acidic conditions, and then between 2.5-2.7 ppm in neutral and basic conditions as shown in the ^{1}H-^{13}C HSQC NMR spectra (see in SI, Figure S8, S11 and S14). These changes are also clearly visible on the ^{13}C NMR spectra at pD 1.4 and 7.6 (see in SI, Figure S6). This variation can be attributed to the deprotonation of the amide function (from [Pd(**oxocyclam**)]$^{2+}$ to [Pd(H$_{-1}$**oxocyclam**)]$^{+}$, which has an important effect in proton nuclei in the vicinity of the amide group. Finally, minor variations in the chemical shifts of β_1, β_2, and the other α protons started to occur at pD ≥ 10.5, indicating minimal changes in the structure of the [Pd(H$_{-1}$**oxocyclam**)]$^{+}$ complexes at high pD.

(25 °C and 80 °C). The following discussion is based on the observations of the ^{1}H NMR spectra at 25 °C, as the same trends were observed at 80 °C. The ^{1}H NMR spectrum of the free ligand recorded at pD = 4.5, corresponding to the doubly protonated H_2L^{2+} species according to the previous potentiometric study, showed a single signal at 2.0 ppm for the two hydrogen atoms in β_1-N position (Figure 5), as well as at 2.8 ppm for the two hydrogen atoms in β_2-N position. However, as soon as the first 0.2 equivalents of Pd(II) were added to the free ligand in solution, two new peaks started to be observed at around 1.5 and 2.1 ppm. These new peaks increased with the addition of larger amounts of Pd(II) salt, while the intensity of the signal of the β_1 hydrogen atoms of the free ligand at 2.0 ppm decreased. The new peaks correspond to the β_1 hydrogen atoms of the [Pd(H$_{-1}$**oxocyclam**)]$^{+}$ complex, ([Pd(**oxocyclam**)]$^{2+}$ not being visible under these conditions. The β_2 protons of the complex appear between 2.5-2.7 ppm. The diastereotopic nature of the β_1 protons is related to their different chemical environments generated by complexation and the rigidity of the complex, which results in different signals for the axial and equatorial β_1 protons. The chair conformation of the six-membered chelate ring formed by coordination of the propylene diamine fragment results in weak ^{3}J coupling involving equatorial-equatorial and axial-equatorial protons, while axial-axial couplings are strong. Thus, the β_1 pseudo-doublet ^{1}H NMR signal at 2.1 ppm can be attributed

to the equatorial proton, which shows strong coupling only with its geminal β_1 proton two bonds away. Conversely, the axial proton at 1.55 ppm is observed as a multiplet as a result of strong $^2J_{ax\text{-}eq}$ (~16 Hz) and $^3J_{ax\text{-}eq}$ (< 4 Hz) couplings.[41] Finally, by reaching a 1:1 Pd(II)/**oxocyclam** ratio, the peak at 2.0 ppm belonging to the free ligand disappears, showing that complexation was complete with stoichiometric amounts of chelator and metal ion.

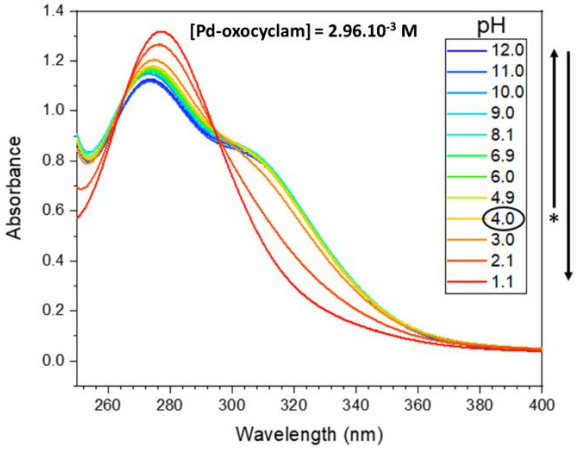

Figure 6. Absorption spectroscopy of Pd(II)-**oxocyclam** (ratio 1:1; [C] = $2.96.10^{-3}$ M) at different pH. The asterisk indicates the pH at which the complexation was performed. Arrows show the sense of variation of the pH during the experiment.

Additional information on the structure of the Pd(II)-**oxocyclam** complex in H_2O was gathered by following the changes with pH of the UV absorption spectra (Figure 6). The spectra recorded at pH ≥ 3 show an absorption maximum at 274 nm (ε ~ 400 $M^{-1}.cm^{-1}$) with a shoulder at 309 nm due to Pd(II) *d*–*d* transitions.[42,43] These spectra can be attributed to the transitions arising from the complex in its fully deprotonated [Pd(H$_{-1}$**oxocyclam**)]$^+$ form. Below pH 3, significant spectral changes are observed, which point to the formation of [Pd(**oxocyclam**)]$^{2+}$ species and probably the protonated species [Pd(H**oxocyclam**)]$^{3+}$ characterized by a more symmetrical absorption band at 279 nm. The position of this band is very similar to that reported for $[Pd(en)_2]^{2+}$ (en = ethylenediamine) at 287 nm.[43,44] We notice that the spectral changes do not provide well-defined isosbestic points, indicating the presence of more than two complex species in equilibrium.

Electrochemistry. Aqueous samples of the Pd(II)-**oxocyclam** complex in 1.0 M KCl electrolyte were prepared at approximately 0.8 mM by adding an acidic $PdCl_2$ solution (1 M in HCl) to a stirred **oxocyclam** solution. After overnight stirring, no precipitation occurred and the pH of each sample was adjusted to pH 2.7 or 5.2 to observe [Pd(**oxocyclam**)]$^{2+}$ and deprotonated [Pd(H$_{-1}$**oxocyclam**)]$^+$ complex species, respectively, based on the speciation diagrams obtained previously by potentiometry. The reduction voltammograms (see in SI, Figure S16) obtained for the sample at pH 2.7 show an irreversible reduction wave (at E_{pc} = −0.55 V *vs.* NHE) and no visible reoxidation wave. Contrastingly, for the sample at pH 5.2 there is no well-defined reduction wave down to the operating limit of the working electrode (at *ca.* −1.4 V), indicating there is no Pd(II) reduction taking place under these conditions. As a comparison, the scarce literature for Pd(II) complexes of tetraazamacrocycles reports reduction potentials ($E_{1/2}$) ranging from −0.63 V to −1.46 V (*vs.* NHE).[45,46] Even if the literature results are not entirely comparable to ours as they were obtained in organic medium (0.1 M ^{n}Bu$_4$NPF$_6$ in MeCN), there is a marked trend of more negative reduction potentials for the least substituted macrocycles that culminates in the most negative value occurring for the complex of **cyclam** ($E_{1/2}$ = −1.46 V). This seemingly corroborates our observation for the [Pd(H$_{-1}$**oxocyclam**)]$^+$ complex species. Regarding the oxidation voltammograms (see in SI, Figure S17), the sample at pH 2.7 displays an irreversible oxidation wave (at E_{pa} = 0.82 V *vs.* NHE) with no visible reduction wave, while for the sample at pH 5.2 there is no defined oxidation wave up to 1.0 V.

Taking into consideration that at pH 5.2 there is only the deprotonated complex species [Pd(H$_{-1}$**oxocyclam**)]$^+$, we may assume that the Pd(II)-**oxocyclam** complex is redox-inert when fully deprotonated (in the voltammetric timescale and used conditions) owing to its overall stability. In contrast, at pH 2.7 there is mainly a mixture of [Pd(**oxocyclam**)]$^{2+}$ and protonated species [Pd(H**oxocyclam**)]$^{3+}$ of the complex that are thermodynamically less stable and structurally less rigid, and so a visible redox activity appears. This corresponds to a reduction potential that is nonetheless rather negative (E_{pc} = −0.55 V *vs.* NHE) and below the estimated threshold for bioreductants (−0.40 V *vs.* NHE), and an oxidation potential that is also rather positive (E_{pa} = 0.82 V *vs.* NHE).

Structural Study. The synthesis of the Pd(II)-**oxocyclam** complex was performed in a refluxing aqueous solution of Na_2PdCl_4 at pH 4 (to avoid precipitation of metal hydroxide) over 16 hours. The complex was obtained as a yellowish powder after purification and characterised by ^{1}H and ^{13}C NMR spectroscopy (see experimental section and SI, Figures S18 and S19). The refluxing conditions ensured the complete formation of the expected complex, irrespective of very fast reaction kinetics.

Single crystals with formula {[Pd(H$_{-1}$**oxocyclam**)]}$_4${[PdCl$_4$]}$_2$·MeOH, suitable for X-ray diffraction studies, were obtained by slow diffusion of diethyl ether vapor into a solution of the complex in methanol. Crystallographic data are reported in SI, Table S1. Crystals contain the [Pd(H$_{-1}$**oxocyclam**)]$^+$ cation (Figure 7a), the square planar $[PdCl_4]^{2-}$ anion and disordered methanol molecules. Furthermore, crystals of the [Pd(**oxocyclam**)]$^{2+}$ complex with formula [Pd(**oxocyclam**)][PdCl$_4$] were obtained by slow evaporation from an aqueous solution of the complex in 1 M HCl (pH < 1) (Figures 7b and c). Crystallographic data are reported in SI, Table S2. The Pd-Cl bond distances in the $[PdCl_4]^{2-}$ complexes present in the two crystals (2.280(2) to 2.3139(10) Å) are similar to those reported for different salts of this complex.[47]

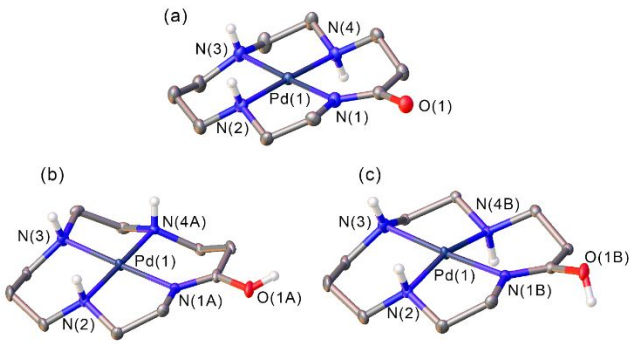

Figure 7. a) View of the structure of the complex cation [Pd(H$_{-1}$**oxocyclam**)]$^{+}$ present in crystals of {[Pd(H$_{-1}$**oxocyclam**)]}$_4${[PdCl$_4$]}$_2$·MeOH in *trans*-III configuration, with atom numbering. The ORTEP plot is at the 50% probability level. **b**) and **c**) Views of the two structures of the complex [Pd(**oxocyclam**)]$^{2+}$ present in crystals of [Pd(**oxocyclam**)][PdCl$_4$] showing *trans*-I and *trans*-III conformations, respectively.

The deprotonated amide donor provides the strongest Pd-N bond in [Pd(H$_{-1}$**oxocyclam**)]$^{+}$ (Figure 7a). The Pd-N$_{amine}$ bond (Pd-N(3)) in *trans* position with respect to the amide donor is slightly elongated, which points to a stronger *trans* effect of the amide donor compared to the amine N atoms. The Pd-N bond distances are very similar to those observed in the solid state for **dioxocyclam** complexes.[48] Two of the three amine N-H groups point to the same side of the macrocycle, while the third points in opposite direction, giving rise to a *trans*-III conformation (*S*,*R*,*R*) by analogy to cyclam complexes.[49]

{[Pd(H$_{-1}$oxocyclam)]}$_4${[PdCl$_4$]}$_2$·MeOH (1A) and [Pd(oxocyclam)][PdCl$_4$] (1B).

	1A		1B
Pd(1)-N(1)	1.987(5)	Pd(1)-N(1A)	2.000(7)
Pd(1)-N(2)	2.048(5)	Pd(1)-N(4A)	2.010(4)
Pd(1)-N(3)	2.051(5)	Pd(1)-N(1B)	2.03(2)
Pd(1)-N(4)	2.028(5)	Pd(1)-N(2)	2.030(3)
		Pd(1)-N(3)	2.047(3)
		Pd(1)-N(4B)	2.119(14)

The presence of the proton on the complex also causes an important increase of the C-O distance from 1.273(7) to 1.336 Å. Besides, an important decrease of the N-C bond is observed from 1.314(8) to 1.280 Å. This clearly indicates that the location of the proton decreases the double bond character of the C-O bond, and increases that of the C-N bond, meaning that the complex evolves towards an iminol, tautomeric form of the amide. This is confirmed by the literature, where it has been shown that in acidic medium, iminol can coordinate to Pd(II) preferentially to the amide oxygen.[50]

A computational study was undertaken to gain information on the structure of the Pd(II)-**oxocyclam** complexes and the effect of protonation on the palladium(II) coordination environment (see in SI, Table S3). A careful investigation of the conformational space for the [Pd(H$_{-1}$**oxocyclam**)]$^{+}$ system provided a minimum energy geometry with the expected square-planar palladium(II) coordination environment, *trans*-III conformation, and bond distances close to those observed in the solid state. The *trans*-I isomer, in which all three amine N-H bonds point to the same side

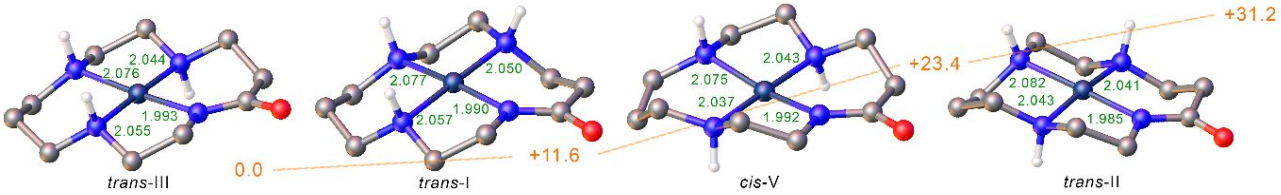

Figure 8. Structures of the [Pd(H$_{-1}$**oxocyclam**)]$^{+}$ complex obtained with DFT calculations showing their relative free energies (in kJ mol^{-1}) and bond distances of the Pd(II) coordination environments (Å).

The structure of the [Pd(**oxocyclam**)]$^{2+}$ complex evidences that the proton is located on the oxygen atom of the ligand (Figures 7b and c). The structure of the cation is disordered into two positions, with the major occupation factors labelled as **A** [0.768(7)] in Figure 7b generating the *trans*-I conformation, in which the three amine N atoms adopt (*S*,*R*,*S*) configurations. The atoms labelled as **B** in Figure 7c display occupation factors of 0.232(7) and generate a complex having *trans*-III conformation (*S*,*R*,*R*). In this complex, a noticeable elongation of the Pd-N$_{amide}$ bond was observed compared to the non-deprotonated complex, from Pd(1)-N(1) = 1.987(5) Å in [Pd(H$_{-1}$**oxocyclam**)]$^{+}$ to Pd(1)-N(1A) = 2.000(7) (*trans*-I) and Pd(1)-N(1B) = 2.03(2) (*trans*-III) in [Pd(**oxocyclam**)]$^{2+}$. All data are summarized in Table 2.

Table 2. Selected bond distances (Å) of the metal coordination environments in

of the macrocycle, has a relative free energy of 11.6 kJ mol^{-1}, and is therefore unlikely to have a significant population in solution. The *trans*-II and *cis*-V isomers have even larger free energy differences with respect to the *trans*-III isomer (Figure 8).

Additional calculations were performed for the [Pd(**oxocyclam**)]Cl$_2$ system [PdL]$^{2+}$. Our calculations indicate that protonation at the carbonyl oxygen atom is favored over protonation of the amide N atom, with the relative free energy of the latter with respect to the former being 6.9 kJ mol^{-1} (see in SI, Figure S20), confirming the iminol form of the Pd(II) complex (Figure 9). Additional protonation of the complex takes place on the amide N atom, resulting in a calculated Pd-N$_{amide}$ distance of 2.274 Å. Thus, these calculations support the model used to analyze the thermodynamic data and the spectral variation observed in the UV absorption spectra, which indicate the

formation of both [Pd(**oxocyclam**)]$^{2+}$ and [Pd(H**oxocyclam**)]$^{3+}$ forms of the complex, very likely while maintaining the square planar N4 coordination around the metal ion. Protonated amide N-coordination in acidic medium is supported by the diastereotopic nature of the ^{1}H NMR signals observed at low pH (Figure 4), as partial ligand decoordination is expected to increase complex flexibility.

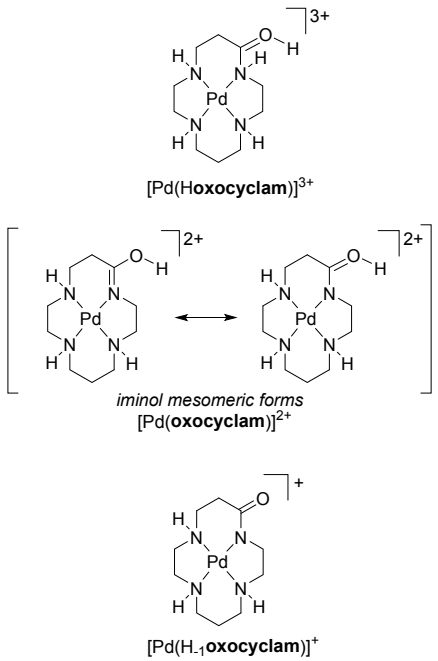

Figure 9. Proposed structures of the different Pd(II)-**oxocyclam** complex species depending on the pH, assumed from studies in solution and in the solid-state, as well as from computational studies.

In conclusion, it can be assumed that the different species can be drawn as proposed in Figure 9. The deprotonated [Pd(H$_{-1}$**oxocyclam**)]$^{+}$ corresponds to the strongest complex in terms of thermodynamic and electrochemical stability. The [Pd(**oxocyclam**)]$^{2+}$ (present under *trans*-I and *trans*-III configurations), less stable than the previous one, can be described by mesomeric forms (amide *vs*. iminol) in which the proton is located on the oxygen atom of the amide function, with a marked tendency towards the iminol form. Finally, the [Pd(H**oxocyclam**)]$^{3+}$ can be represented with a proton on both the oxygen and the nitrogen atoms. This species is formed in solution at pH < 4 (Figure 3), with complex dissociation taking place simultaneously.

^{109}Pd-radiolabeling. The radiolabeling of **oxocyclam** and its conjugable version, ***p*-H$_2$N-Bn-oxocyclam,** with palladium-109 was investigated in different media, with varying pH and temperatures. The aim was to confirm that the *C*-functionalization does not affect the "original" complexing structure of **oxocyclam,** which retains its coordination properties intact in terms of labeling efficiency, and to obtain preliminary radiolabeling results that are necessary for the future use of this chelator in nuclear medicine applications.

^{109}Pd-labeling of both ligands was then investigated for 10 minutes in: *i*) 0.1 M NH_4OAc at various pH values (3.5, 7.0 and 8.5) at 90 °C, *ii*) 0.1 M NH_4OAc at pH 3.5 at 25 °C and *iii*) 0.01 M PBS at pH 7.0 at the same temperatures (25 °C and 90 °C). For each complexation condition, a ligand/radiometal molar ratio of 2:1 was used to ensure maximum metal complexation, as reported in our previous study[30] and as calculated from the initial mass of the irradiated ^{108}Pd-target. The radiochromatograms of the ^{109}Pd-nuclide are shown for reference in the two media used (NH_4OAc or PBS) in Figure S21.

Oxocyclam was successfully radiolabeled in NH_4OAc at pH 3.5 under heating at 90 °C for 10 minutes with a labeling efficiency (LE) greater of 99%. When the reactions were carried out at the same temperature but with more basic pH values (7.0 and 8.5), a sharp drop in labeling efficiency was observed (LE ≤ 53%). (Figure 10). These results are comparable to radiolabeling trends for other macrocyclic cyclam derivatives in which radiolabeling efficiencies decrease with increasing pH, most likely as a result of palladium hydroxide precipitation.[30]

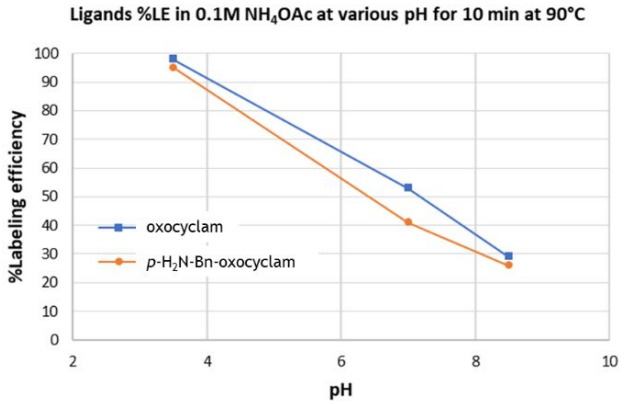

Figure 10. Labeling efficiency (%LE) for ^{109}Pd-labeling of **oxocyclam** and ***p*-H$_2$N-Bn-oxocyclam** in 0.1 M NH_4OAc at 90 °C for 10 minutes at pH 3.5, 7.0 and 8.5.

Interestingly, three radiolabeled species were identified when the complexation of **oxocyclam** was performed at pH 3.5, against two species at pH 7.0 and 8.5 (Figure 11). Labeling was then repeated for 10 minutes in NH_4OAc at the optimum pH 3.5 at 25 °C. Under these conditions, the [^{109}Pd]Pd-**oxocyclam** complex was also obtained with a very high labeling yield (LE ≥ 98%) (see in SI, Figure S22), as previously seen at high temperature. Whether at 25 °C or 90 °C, **oxocyclam** complexation at pH 3.5 provided three species with no significant change in their proportions.

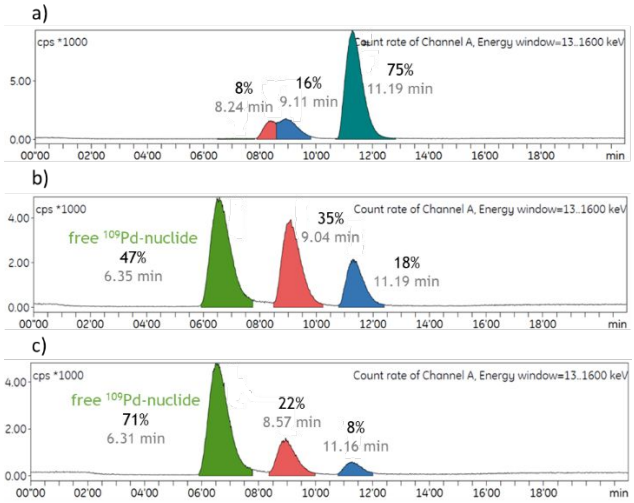

Figure 11. Radio-HPLC chromatograms for ^{109}Pd-labeling of **oxocyclam** in 0.1 M NH_4OAc at 90 °C for 10 minutes: **a**) at pH 3.5, **b**) at pH 7.0 and **c**) at pH 8.5.

The radiolabeling of **oxocyclam** was then studied in PBS (pH 7), for 10 minutes at 25 °C and 90 °C. Whatever the temperature, radiolabeling was very efficient with a LE greater than 98%, probably as a result of the PBS buffer preventing extensive precipitation of palladium hydroxide.[30] At room temperature, two major species were identified for the ^{109}Pd-based **oxocyclam** complex with quasi-similar proportions (42% and 55%), whereas at 90 °C the same two species were observed with very different proportions (82% and 16% respectively) (see in SI, Figure S23).

Regarding the nature of the **oxocyclam** species observed in the radiochromatograms, the equilibrium studies reported above indicate that three species are present in solution at pH 3.5, and thus most likely different protonated forms and/or different configurations of a complex are responsible for the three radiospecies observed. At pH 7, thermodynamic studies indicate that the $[Pd(H_{-1}$**oxocyclam**$)]^+$ species is the only one with a significant population. In contrast, some radiochromatograms show more than one Pd(II)-radiocomplex at pH 7 (either in PBS or NH_4OAc and at 25 °C or 90 °C). Thus, we can conclude that thermodynamic *trans*-III species and kinetic species such as *trans*-I, *trans*-II and *cis*-V isomers are probably the cause of the observed behavior. This is supported by the characterization of the Pd(II)-**oxocyclam** complex by ^{13}C NMR spectroscopy (see Experimental part and SI, Figures S18 and S19) that revealed two main species as well as an additional set of signals due to a minor species, especially in the range 50-60 ppm (CH_2 α-N) (see SI, Figure S19), most likely corresponding to these different configurational isomers. These latter can be formed under the radiolabeling conditions at pH 7, and their subsequent evolution into the thermodynamic *trans*-III product is easy for **oxocyclam** species (Figure S23). This process can occur in neutral solution but seems inhibited in acidic solution (Figures 11a and S22). A similar slow isomer interconversion has been observed by others, for example in the case of a $[Zn(cyclam)]^{2+}$ complex, with thermodynamic equilibrium only being reached after several hours.[51]

In order to study the influence of the *C*-functionalization of **oxocyclam** on ^{109}Pd-complexation, the radiolabeling of ***p*-H_2N-Bn-oxocyclam** was performed in the same conditions described previously. As expected, ^{109}Pd-labeling was more efficient at pH of 3.5 than at 7.0 and 8.5, in NH_4OAc, after 10 minutes at 90 °C (Figure 10). Interestingly, a single radiocomplex was obtained at neutral and basic pHs *vs.* three species at pH 3.5 (Figure 12). The labeling at pH 3.5 at 25 °C also led to three radiocomplexes, but with a modification in the species ratio and retention times compared to 90 °C, while retaining a remarkable labeling efficiency (see in SI, Figure S24 for 25 °C, and Figure 12a for 90 °C).

For the complex formed in PBS at pH 7 for 10 minutes, the number of species decreased upon heating at 90 °C from three to one (see in SI, Figure S25). After 24 hours at room temperature, this single radiocomplex was reanalyzed and the chromatogram showed three peaks (see in SI, Figure S26).

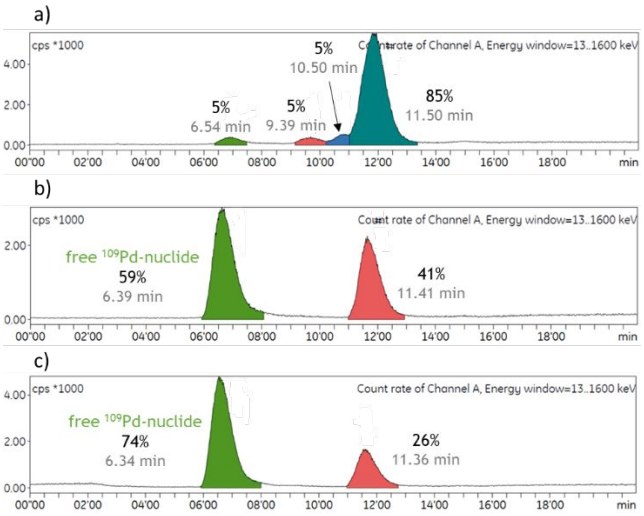

Figure 12. Radio-HPLC chromatograms for ^{109}Pd-labeling of ***p*-H_2N-Bn-oxocyclam** in 0.1 M NH_4OAc at 90 °C for 10 minutes: **a**) at pH 3.5, **b**) at pH 7.0 and **c**) at pH 8.5.

In contrast with the results obtained using NH_4OAc, the PBS solution induce a different number of species formed between ***p*-H_2N-Bn-oxocyclam** and **oxocyclam** (Table 3). The presence of the additional organic moiety likely has an impact on the conformation of the ligand at neutral pH, affecting the complexation reaction. Nevertheless, the presence of the *C*-appended function incorporated into **oxocyclam** maintains its radiolabeling efficiency.

The results obtained for **oxocyclam** were compared with those of **cyclam,** whose coordination with palladium-109 was previously studied by our group.[30] Our investigations showed that **cyclam** radiolabeling in NH_4OAc at pH 3.5 for 10 minutes led to single complex species with LE of 38% at room temperature and 42% at 90 °C. Despite a high LE of 98% in PBS (pH 7, 10 min) at 90 °C, the value decreased to only 38% at room temperature. According to these results, **oxocyclam** showed better Pd(II) chelating properties than **cyclam** in terms of complexation kinetics.

Table 3. Radiolabeling in 0.1 M NH_4OAc (pH 3.5) and 0.01 M PBS (pH 7) for 10 min at 25 °C and 90 °C.

		Oxocyclam	***p*-H_2N-Bn-oxocyclam**
Medium	T (°C)	Number of species (ratio%)	Number of species (ratio%)
NH_4OAc (pH 3.5)	25	3 (20/15/63)	3 (23/41/33)
	90	3 (8/16/75)	3 (5/5/85)
PBS (pH 7)	25	2 (2/42/55)	3 (6/16/77)
	90	2 (82/16)	1 (99)

The stability of [^{109}Pd]Pd-**oxocyclam** and [^{109}Pd]Pd-***p*-H_2N-Bn-oxocyclam** radiocomplexes was studied by assessing their transchelation using an excess of a solution of 1.0 M EDTA (1000 equivalents, pH 14) over a period of 24 hours (in 0.01 M PBS, pH 7, 25 °C) (see in SI, Figures S27 and S28). A moderate transchelation towards EDTA (7-9%) was observed for both radiocomplexes after 24 hours. Under the same conditions, the [^{109}Pd]Pd-**cyclam** complex was slightly less inert with a transchelation of approximately 13% as previously reported.[30] Interestingly, the addition of EDTA to [^{109}Pd]Pd-***p*-H_2N-Bn-oxocyclam** in solution induced a modification in the number of species from three to one clearly visible after 1 h and 24 h (see in SI, Figures S28). It is possible that carboxylate groups from EDTA stabilize one configuration in solution through hydrogen bonds as reported for a phthalate Zn(II) cyclam complex.[51]

CONCLUSIONS

The main challenges in the complexation of palladium(II) relate to the need for selective ligands, the stability of the complexes under various reaction conditions, and addressing concerns related to atom economy, toxicity, and sustainability. The design of efficient ligands and the control of steric and electronic factors are essential to achieve the desired reactivity in different applications such as palladium-catalyzed reactions or radiolabeling with palladium radionuclides in nuclear medicine. Cyclam derivatives have proven to be very attractive for the complexation of palladium(II) due to their ability to provide selective and stable coordination environments, thereby influencing reactivity and enabling the development of these applications. Due to their particular acid-base properties, specifically from their amide function(s), oxocyclam derivatives offer a similarly interesting potential. Our study investigates the intricate coordination of **oxocyclam** with palladium(II) and introduces a novel bifunctional analogue featuring an aniline pendant, ***p*-H_2N-Bn-oxocyclam**. The research presents a multifaceted examination of the Pd(II)-**oxocyclam** complex using various analytical techniques. The convergence of information highlighted the presence of [Pd(H**oxocyclam**)]$^{3+}$, [Pd(H$_{-1}$**oxocyclam**)]$^{+}$ and [Pd(**oxocyclam**)]$^{2+}$ complexes, with two different configurations in the latter case, and the evidence of the protonation of the oxygen atom rather than the nitrogen of the amide function, giving rise to an interesting species of iminol complex. The critical structural details highlighted the robustness of the Pd-N bonds and the impact of protonation on the geometry of the complex. Whatever the structure, the complexes are inert and thermodynamically stable, paving the way for their use in a variety of applications, especially through the new bifunctional analogue. Radiolabeling experiments with **oxocyclam** and its analogue demonstrated exceptional efficiency at pH 3.5, highlighting the importance of pH in optimizing labeling yields. The variations observed in the radiolabeled species at different pH values provide valuable information for understanding the dynamics of complexation. The stability studies, including transchelation experiments with EDTA, revealed the robustness of the [^{109}Pd]Pd-**oxocyclam** and [^{109}Pd]Pd-***p*-H_2N-Bn-oxocyclam** radiocomplexes. The synthesis of the bifunctional analogue expands the scope of potential applications, not only for ^{109}Pd-coordination but also for ^{99m}Tc-radiolabelling considering the affinity of **oxocyclam** for ^{99m}Tc-complexation, thus offering a promising route for further exploration of this chelator with various metals in coordination chemistry and radiopharmaceutical development.

EXPERIMENTAL SECTION

Material. Classical reagents were purchased from AC Organics, TCI, ALDRICH Chemical Co, and Easy Chelators. **Oxocyclam** was purchased from Chematech.

Compound **1** was synthesized as previously described and the ^{1}H and ^{13}C NMR shifts and spectra are given in the ESI. NMR data were recorded at the "services communs" of the University of Brest. ^{1}H and ^{13}C NMR spectra were recorded using Bruker Avance 500 (500 MHz) or Bruker AMX-3 300 (300 MHz) spectrometers. The δ scales are relative to TMS (^{1}H and ^{13}C NMR spectra). The signals are described as follows: chemical shift, multiplicity (s, singlet; br s, broad singlet; d, doublet; t, triplet; m, multiplet), coupling constants J in hertz (Hz), assignment: CH_2 α-N and CH_n β-N (n = 1 or 2) corresponding to CH or CH_2 located in alpha or beta position of the considered nitrogen atom, respectively; the type of nuclei is indicated in italic; *Ar* is a generic term used in subscript for all hydrogen or carbon aromatic atoms; Ph is the abbreviation for a C_6H_5 group; $PhNO_2$ and $PhNH_2$ correspond to the aromatic part of the C-functionalization in its different forms; HRMS spectra were recorded at the HRMS platform of the University of Orleans, France (FR 2708 CBM-ICOA).

***p*-H_2N-Bn-oxocyclam. Compound 4** (0.2 g, 0.488 mmol, 1 eq) was dissolved in EtOH (20 mL), and palladium on activated charcoal 10% (0.78 g, 1.5 eq Pd) was added to this solution. The mixture was stirred vigorously under a hydrogen atmosphere for 1 day. The mixture was filtered through Celite® and the solvent was evaporated under reduced pressure. The crude product was purified on reverse phase C18 HPLC (H_2O/CH_3CN from 0 to 80% CH_3CN) yielding ***p*-H_2N-Bn-oxocyclam** as yellow powder (0.136 g, 0.426 mmol, 87 %). ^{1}H NMR (400 MHz, MeOD-d^4) δ (ppm): 7.40 (d, J = 8.5 Hz, 2H, CH_{Ar} $PhNH_2$), 7.36 (d, J = 8.5 Hz, 2H, CH_{Ar} $PhNH_2$), 3.88-3.78 (m, 1H), 3.50 (dt, J = 12.0, 5.4 Hz, 1H), 3.42 (s, 2H), 3.35 (d, J = 4.3 Hz, 1H), 3.32-3.28 (m,

4H), 3.28-3.23 (m, 2H), 3.23-3.19 (m, 2H), 3.18 (s, 3H), 3.09 (dd, J = 13.6, 6.6 Hz, 1H), 2.90 (dd, J = 13.6, 7.9 Hz, 1H), 2.19-2.00 (m, 2H, CH_2 β-N). ^{13}C NMR (126 MHz, MeOD-d^4) δ (ppm): 176.4 (*C*O), 138.6 (C_{Ar} PhNH$_2$), 132.7 (C_{Ar} PhNH$_2$), 131.8 (CH$_{Ar}$ PhNH$_2$), 123.6 (CH$_{Ar}$ PhNH$_2$), [48.1, 47.6, 47.4, 46.8] (*C*H$_2$ α-N), 46.1 (*C*H β-N), [45.7, 37.4] (*C*H$_2$ α-N), 37.0 (*C*H$_2$-PhNH$_2$), 25.1 (*C*H$_2$ β-N). FT-IR (cm^{-1}, ATR): N-H (primary amine): 3348-3427, N-H (secondary amine): 3262, C=O (amide): 1614-1656. HRMS (ESI+) m/z: [$C_{17}H_{30}N_5O$] = [M+H]$^+$ = 320.2444 (cal. 320.2444).

Complexation of palladium(II) with oxocyclam.

Synthesis. The **oxocyclam** ligand (81 mg, 0.378 mmol, 1 eq) was dissolved in water (6 mL) and the pH of the solution was adjusted to 4 using HCl solution before the addition of 1.4 eq of Na_2PdCl_4 in water (6.6 mL). The reaction was refluxed overnight during which the pH was readjusted to 4 by addition of NaOH solution. The mixture was then stirred overnight under reflux. After cooling to room temperature, solid impurities were filtered off and the solution was evaporated under vacuum. The residue was dissolved in a minimal amount of dry methanol. The insoluble salts formed were filtered off and the filtrate was evaporated to dryness to afford a yellowish powder. This procedure was repeated until no more salts were present. ^{1}H NMR (500 MHz, D_2O, 25 °C, pD = 7.0) δ (ppm): ^{1}H NMR (400 MHz, D_2O) δ 5.32-5.03 (m, 2H, N*H*), 3.61-3.51 (m, 1H, CH_2α-NCO), 3.41-2.45 (m, 15H, CH_2α-NCO, CH_2α-N, CH_2α-CO), 2.25-2.12 (m, 1H, CH_2β-N), 1.80-1.59 (m, 1H, CH_2β-N). ^{13}C NMR (125 MHz, D_2O, 25 °C, pD = 7.0) δ (ppm): [175.7, 175.3] (*C*O), [58.9, 58.7, 58.1, 58.0, 56.8, 56.7, 56.2, 56.0, 55.8, 55.4, 55.3, 54.8, 54.7, 54.3, 53.7, 53.5, 53.4, 52.0, 51.9, 51.8, 51.4] (*C*H$_2$αN) [40.5, 40.2 (x 2)] (*C*H$_2$α-CO), [32.0, 31.6] (*C*H$_2$β-N) [two series of peaks are clearly visible: *trans*-III and *trans*-I configurations, plus one very minor series visible between 50-60 ppm which can be attributed to *cis*-V or *trans*-II configuration, as suggested by the DFT calculation. Each series was not identified separately due to the overlap of the signals].

Potentiometry. The potentiometric titrations were performed in aqueous solution at 25.0 ºC and 1.0 M KCl, using the potentiometric setup and methods previously described.[52] A stock solution of **oxocyclam** was prepared at 2.0 mM in water (acidified to *ca.* pH 2 with HCl), and a stock solution of palladium(II) chloride was prepared at 25 mM in 1.0 M HCl. Titrations were run containing *ca.* 0.04 mmol of ligand, and palladium(II) was added at 0.8 equiv. in complexation titrations. All titrations were run in-cell without the need for any out-of-cell measurements. Nonetheless, during titrations with Pd(II) the equilibrium was attained rather slowly in the region of pH = 2.5–7.0, which required the use of especially long waiting times (*ca.* 1 hour per point) in data acquisition in this region. Only mononuclear complex species could be found in the experimental conditions used.

The overall equilibrium constants $\beta_{M_mH_hL_l}$ were determined in log units from fitting of the potentiometric titrations as defined by $\beta_{M_mH_hL_l} = [M_mH_hL_l]/[M]^m[H]^h[L]^l$, while stepwise constants are defined by $K_{M_mH_hL_l} = [M_mH_hL_l]/[M_mH_{h-1}L_l][H]$ and were calculated from the difference in log units between overall constants of sequentially protonated species. The potentiometric titrations were fitted with the Hyperquad 2008 software.[53] The overall equilibrium constants and the corresponding stepwise constants are collected in Table 1. The errors quoted are the standard deviations calculated by the fitting program for the experimental data in each system. The value of $K_w = [H^+][OH^-]$ was taken from the literature as equal to $10^{-13.75}$.[54] Stability constants of the palladium(II) chloride complexes (PdCl, $PdCl_2$, $PdCl_3$, and $PdCl_4$) were taken from the literature and used during data fitting.[55]

Electrochemistry. Aqueous samples of the Pd(II)-**oxocyclam** complex in 1.0 M KCl electrolyte were prepared at *ca.* 0.8 mM by addition of an acidic $PdCl_2$ solution (1.0 M in HCl) to a stirred solution of **oxocyclam**. After overnight stirring the solution changed from yellow to colorless, and the pH of each sample was adjusted by slow addition of a KOH solution. Samples were prepared at pH 2.7 and 5.2 to observe protonated and fully deprotonated complex species, respectively, according to the speciation diagrams previously obtained by potentiometry.

Cyclic voltammograms were run on a BAS CV-50W voltammetric analyzer with a BAS C-2 cell stand. A custom 1 mL closed glass cell was fitted with a three-electrode setup consisting of a glassy carbon working electrode, a platinum wire counter-electrode, and Ag/AgCl reference electrode filled with 3 M KCl solution. Voltammograms were run under nitrogen at a scan rate of 100 mV/s towards either reduction or oxidation of Pd(II), respectively by ramping the potential downwards or upwards from 0 V. The redox potential values were converted to the NHE reference (+0.222 V relative to the Ag/AgCl reference electrode used).

DFT calculations. Density functional theory (DFT) calculations were performed with the wB97XD functional, which incorporates empirical dispersion,[56,57] and the Gaussian 16 program package.[58] Relativistic effects were considered with the use of the relativistic pseudopotential ECP28MDF, which incorporates the 28 inner electrons of Pd in the core, and the associated triple-ξ valence basis set.[59] The Def2-TZVPP basis set was used for all other atoms.[60] Geometry optimizations were carried out incorporating solvent effects (water) with the integral equation formalism variant of the polarized continuum model (PCM).[61,62] Frequencies were obtained using analytical second derivatives to confirm the nature of the optimized geometries as local energy minima. A superfine integration grid was used throughout.

X-ray Diffraction Determination. X-ray diffraction was determined at the University of Rennes. Suitable crystal for X-ray diffraction single crystal experiments were selected and mounted on the goniometer head of a D8 Venture (Bruker-AXS) diffractometer equipped with a CMOS-PHOTON70 detector, using Mo-Kα radiation (λ = 0.71073 Å, graphite monochromator) at T = 150(2) K. Crystal structure was solved by dual-space algorithm using SHELXT program,[63] and then refined with full-matrix least-squares methods based on F2 (SHELXL).[64] All non-Hydrogen atoms

were refined with anisotropic atomic displacement parameters. CCDC 2337540 and 2337541 contain the supplementary crystallographic data for this paper. These data can be obtained free of charge from The Cambridge Crystallographic Data Centre via www.ccdc.cam.ac.uk/data_request/cif.

^{109}Pd-radiolabeling. The ^{109}Pd-stock solution for radiolabeling was produced and purified according the method as previously described.[30] All solvents used were HPLC grade (Merck KGaA, Darmstadt, Germany,) and all buffer solutions were prepared using Milli-Q grade water (>18 MΩ/cm). The activity of the $[^{109}Pd][PdCl_4]^{2-}$ solution and ^{109}Pd-chelator complexes were measured using a Capintec CRC-15R gamma detector (Capintec Inc., Florham Park, NJ, USA) (isotope measurement number 435 × 10). All radiolabeled compounds were analyzed by radio-HPLC analysis on Agilent 1260 Infinity II HPLC apparatus (Agilent Technologies, CA, USA) fitted with a radiometric GABI Star gamma detector (raytest GmbH, Straubenhardt, Germany). The radio-HPLC was run using an Agilent Zorbax Eclipse Plus-C18 column (5 µm; 4.6 × 250 mm) with a gradient elution over 21 min using H_2O (0.1% TFA) (solvent A) and MeCN (0.1% TFA) (solvent B) with 5% of B over 2 min, 5% → 95% of B over 15 min, 95% of B over 2 min and 95% → 5% of B over 2 min, flow rate of 1 mL/min.

$[^{109}Pd][PdCl_4]^{2-}$ solution (9.3 µmol/mL; 10-43 µL; 10-22 MBq) was added to the appropriate volume of chelator (**oxocyclam** or ***p*-H$_2$N-Bn-oxocyclam**) (5.4-6.3 µmol/mL) dissolved in 0.1 M NH_4OAc buffer or 0.01 M PBS buffer for an approximate molar equivalent of chelator/metal 2:1 and a final reaction volume of 300 µL.

The ^{109}Pd-radiolabeling for both ligands was performed in 0.1 M NH_4OAc for 10 min at 90 °C at pH = 3.5, 7 or 8.5. The radiolabeling was then carried out in the same solvent for 10 min at 25 °C at the optimal pH of 3.5.

The ligands were radiolabeled in 0.01 M PBS at pH 7 for 10 min at 90 °C and 25 °C. Radio-HPLC analysis was performed on the reaction solution in order to determine the radiolabelling efficiency (%).

EDTA challenge. Oxocyclam and **H$_2$N-Bn-oxocyclam** were radiolabeled as described above in PBS buffer (0.01 M, pH 7). The $[^{109}Pd]PdCl_4]^{2-}$ solution (100-200 µL, 10-12 MBq of chelator) was added to the chelator solution (chelator/metal 2:1). The reaction was performed at 25 °C for 10 minutes. Radio-HPLC analysis was done to confirm labeling, followed by addition of EDTA solution (1.0 M, 400 µl, 1000 eq, pH 14) to each reaction vial. The reaction solutions were left at room temperature (25 °C) with radio-HPLC monitoring at 1 h and 24 h.

ASSOCIATED CONTENT

Supporting Information. 1H, 13C, 2D NMR spectra, HRMS spectra, species distribution diagrams, cyclic voltamograms, crystallographic data, DFT calculation, radio-HPLC. This material is available free of charge via the Internet at http://pubs.acs.org."

AUTHOR INFORMATION

Corresponding Author

* raphael.tripier@univ-brest.fr
* nathalie.lebris@univ-brest.fr

Author Contributions

The manuscript was written through contributions of all authors. / All authors have given approval to the final version of the manuscript. / ‡These authors contributed equally. (match statement to author names with a symbol)

Funding Sources

Part of this research was funded by the ANR program ThromPET (ANR-21-CE19-0021).

ACKNOWLEDGMENT

R.T. and N.L.B. acknowledge the Ministère de l'Enseignement Supérieur et de la Recherche and the Centre National de la Recherche Scientifique. C.H.S.D thanks the South African Nuclear Energy Corporation for financial support and palladium target irradiation. C.P.-I. and D. E.-G. thank Centro de Supercomputación de Galicia for providing access to computing facilities and Ministerio de Ciencia e Innovación (Grant PID2022-138335NB-I00) and Xunta de Galicia (ED431C 2023/33) for generous financial support. L.M.P.L was financially supported by FCT - Fundação para a Ciência e a Tecnologia, I.P., through MOSTMICRO-ITQB R&D Unit (UIDB/04612/2020, UIDP/04612/2020) and LS4FUTURE Associated Laboratory (LA/P/0087/2020).

REFERENCES

(1) Kirschner, S.; Wei, Y. K.; Francis, D.; Bergman, J. G. Anticancer and Potential Antiviral Activity of Complex Inorganic Compounds. *J. Med. Chem.* **1966**, *9* (3), 369–372. https://doi.org/10.1021/jm00321a026.

(2) Marques, M. P. M. Platinum and Palladium Polyamine Complexes as Anticancer Agents: The Structural Factor. *Int. Sch. Res. Notices.* **2013**, *2013*, e287353. https://doi.org/10.1155/2013/287353.

(3) Carneiro, T. J.; Martins, A. S.; Marques, M. P. M.; Gil, A. M. Metabolic Aspects of Palladium(II) Potential Anti-Cancer Drugs. *Front. Oncol.* **2020**, *10*, 590970. https://doi.org/10.3389/fonc.2020.590970.

(4) Graham, R. D.; Williams, D. R. The Synthesis and Screening for Anti-Bacterial, -Cancer, -Fungicidal and -Viral Activities of Some Complexes of Palladium and Nickel. *J. Inorg. Nucl. Chem.* **1979**, *41* (8), 1245–1249. https://doi.org/10.1016/0022-1902(79)80496-0.

(5) Vakrat-Haglili, Y.; Weiner, L.; Brumfeld, V.; Brandis, A.; Salomon, Y.; Mcllroy, B.; Wilson, B. C.; Pawlak, A.; Rozanowska, M.; Sarna, T.; Scherz, A. The Microenvironment Effect on the Generation of Reactive Oxygen Species by Pd–Bacteriopheophorbide. *J. Am. Chem. Soc.* **2005**, *127* (17), 6487–6497. https://doi.org/10.1021/ja046210j.

(6) Fawwaz, R. A.; Hemphill, W.; Winchell, H. S. Potential Use of ^{109}Pd-Porphyrin Complexes for Selective Lymphatic Ablation. *J. Nucl. Med.* **1971**, *12* (5), 231–236.

(7) Doi, J. D.; Lavallee, D. K.; Srivastava, S. C.; Prach, T.; Richards, P.; Fawwaz, R. A. Preparation of ^{109}Pd-Hematoporphyrin for Selective Lymphatic Ablation Using *N*-Methylhematoporphyrin. *Int. J. Appl. Radiat. Isotopes* **1981**,

32 (12), 877–880. https://doi.org/10.1016/0020-708X(81)90071-5.

(8) Peschel, R. E.; Colberg, J. W.; Chen, Z.; Nath, R.; Wilson, L. D. Iodine-125 Versus Palladium-103 Implants for Prostate Cancer: Clinical Outcomes and Complications. *J. Cancer.* **2004**, *10* (3), 170.

(9) Bagshaw, H. P.; Williams, N. L.; Huang, Y. J.; Tward, J. D.; Gaffney, D. K. Palladium Interstitial Implant in Combination with External Beam Radiotherapy and Chemotherapy for the Definitive Treatment of a Female Urethral Carcinoma. *Gynecol. Oncol. Rep* **2015**, *13*, 40–43. https://doi.org/10.1016/j.gore.2015.06.001.

(10) Van Rooyen, J.; Szucs, Z.; Rijn Zeevaart, J. A Possible *in Vivo* Generator ^{103}Pd/^{103m}Rh—Recoil Considerations. *Appl. Radiat. Isot.* **2008**, *66* (10), 1346–1349. https://doi.org/10.1016/j.apradiso.2008.02.088.

(11) Filosofov, D.; Kurakina, E.; Radchenko, V. Potent Candidates for Targeted Auger Therapy: Production and Radiochemical Considerations. *Nucl. Med. Biol.* **2021**, *94–95*, 1–19. https://doi.org/10.1016/j.nucmedbio.2020.12.001.

(12) Funkhouser, J. Reinventing Pharma: The Theranostic Revolution. *Curr. Drug Discov.* **2002**, 17–19.

(13) Wadas, T. J.; Wong, E. H.; Weisman, G. R.; Anderson, C. J. Coordinating Radiometals of Copper, Gallium, Indium, Yttrium, and Zirconium for PET and SPECT Imaging of Disease. *Chem. Rev.* **2010**, *110* (5), 2858–2902. https://doi.org/10.1021/cr900325h.

(14) Boros, E.; Packard, A. B. Radioactive Transition Metals for Imaging and Therapy. *Chem. Rev.* **2019**, *119* (2), 870–901. https://doi.org/10.1021/acs.chemrev.8b00281.

(15) Kostelnik, T. I.; Orvig, C. Radioactive Main Group and Rare Earth Metals for Imaging and Therapy. *Chem. Rev.* **2019**, *119* (2), 902–956. https://doi.org/10.1021/acs.chemrev.8b00294.

(16) W. Price, E.; Orvig, C. Matching Chelators to Radiometals for Radiopharmaceuticals. *Chem. Soc. Rev.* **2014**, *43* (1), 260–290. https://doi.org/10.1039/C3CS60304K.

(17) Vivier, D.; Sharma, S. K.; Zeglis, B. M. Understanding the *in Vivo* Fate of Radioimmunoconjugates for Nuclear Imaging. *J. Label. Compd. Radiopharm.* **2018**, *61* (9), 672–692. https://doi.org/10.1002/jlcr.3628.

(18) Bartholomä, M. D. Recent Developments in the Design of Bifunctional Chelators for Metal-Based Radiopharmaceuticals Used in Positron Emission Tomography. *Inorg. Chim. Acta.* **2012**, *389*, 36–51. https://doi.org/10.1016/j.ica.2012.01.061.

(19) Lelong, E.; Suh, J.-M.; Kim, G.; Esteban-Gómez, D.; Cordier, M.; Lim, M. H.; Delgado, R.; Royal, G.; Platas-Iglesias, C.; Bernard, H.; Tripier, R. Complexation of *C*-Functionalized Cyclams with Copper(II) and Zinc(II): Similarities and Changes When Compared to Parent Cyclam Analogues. *Inorg. Chem.* **2021**, *60* (15), 10857–10872. https://doi.org/10.1021/acs.inorgchem.1c01572.

(20) Camus, N.; Halime, Z.; Le Bris, N.; Bernard, H.; Beyler, M.; Platas-Iglesias, C.; Tripier, R. A [Two-Step/One Week] Synthesis of *C*-Functionalized Homocyclens and Cyclams. Application to the Preparation of Conjugable BCAs without Chelating Properties Alteration. *RSC Adv.* **2015**, *5* (104), 85898–85910. https://doi.org/10.1039/C5RA17133D.

(21) Fawwaz, R. A.; Wang, T. S.; Srivastava, S. C.; Rosen, J. M.; Ferrone, S.; Hardy, M. A.; Alderson, P. O. Potential of Palladium-109-Labeled Antimelanoma Monoclonal Antibody for Tumor Therapy. *J. Nucl. Med.* **1984**, *25* (7), 796–799.

(22) Das, T.; Chakraborty, S.; Sarma, H. D.; Banerjee, S. A Novel [^{109}Pd] Palladium Labeled Porphyrin for Possible Use in Targeted Radiotherapy. *Radiochim. Acta.* **2008**, *96* (7), 427–433. https://doi.org/10.1524/ract.2008.1505.

(23) Chakraborty, S.; Das, T.; Sarma, H. D.; Banerjee, S. Effect of Lipophilicity on Biological Properties of ^{109}Pd-Porphyrin Complexes: A Preliminary Investigation. *J. Porphyr. Phthalocyanines* **2012**, *16* (01), 64–71. https://doi.org/10.1142/S1088424611004427.

(24) Albéniz, A. C.; Espinet, P. Palladium: Inorganic & Coordination Chemistry. In *Encyclopedia of Inorganic Chemistry*; John Wiley & Sons, Ltd, 2006. https://doi.org/10.1002/0470862106.ia178.

(25) Kapdi, A. R.; Fairlamb, I. J. S. Anti-Cancer Palladium Complexes: A Focus on PdX_2L_2, Palladacycles and Related Complexes. *Chem. Soc. Rev.* **2014**, *43* (13), 4751–4777. https://doi.org/10.1039/C4CS00063C.

(26) Bazzicalupi, C.; Bencini, A.; Bianchi, A.; Giorgi, C.; Valtancoli, B. Pd(II) Complexes of Aliphatic Polyamine Ligands in Aqueous Solution: Thermodynamic and Structural Features. *Coord. Chem. Rev.* **1999**, *184* (1), 243–270. https://doi.org/10.1016/S0010-8545(99)00003-X.

(27) De Stefano, C.; Gianguzza, A.; Pettignano, A.; Sammartano, S. Palladium(II) Complexes of Aminopolycarboxylic Ligands in Aqueous Solution. *J. Chem. Eng. Data* **2011**, *56* (12), 4759–4771. https://doi.org/10.1021/je200759g.

(28) Le Bris, N.; Pineau, J.; Lima, L. M. P.; Tripier, R. Palladium(II) Coordination with Polyazacycloalkanes. *Coord. Chem. Rev.* **2022**, *455*, 214343. https://doi.org/10.1016/j.ccr.2021.214343.

(29) Harrington, J. M.; Jones, S. B.; Hancock, R. D. Determination of Formation Constants for Complexes of Very High Stability: Logβ_4 for the $[Pd(CN)_4]^{2-}$ Ion. *Inorg. Chim. Acta.* **2005**, *358* (15), 4473–4480. https://doi.org/10.1016/j.ica.2005.06.081.

(30) Pineau, J.; Lima, L. M. P.; Platas-Iglesias, C.; Zeevaart, J. R.; Driver, C. H. S.; Le Bris, N.; Tripier, R. Relevance of Palladium to Radiopharmaceutical Development Considering Enhanced Coordination Properties of TE1PA. *Chem. Eur. J.* **2022**, *28* (41), e202200942. https://doi.org/10.1002/chem.202200942.

(31) Kimura, E.; Korenari, S.; Shionoya, M.; Shiro, M. The First X-Ray Crystal Structures of the Platinum(II)-in and -out Complexes with Dioxocyclams. *J. Chem. Soc., Chem. Commun.* **1988**, No. 17, 1166–1168. https://doi.org/10.1039/C39880001166.

(32) Bu, X. H.; An, D. L.; Cao, X. C.; Zhang, R. H.; Clifford, T.; Kimura, E. New Dioxocyclam Ligands Appended with 2-Pyridylmethyl Pendant(s): Synthesis, Properties and Crystal Structure of Their Copper(II) Complexes (Dioxocyclam = 1,4,8,11-Tetraazacyclotetradecane-12,14-Dione). *J. Chem. Soc., Dalton Trans.* **1998**, No. 13, 2247–2252. https://doi.org/10.1039/A802327A.

(33) Kurosaki, H.; Yoshida, H.; Fujimoto, A.; Goto, M.; Shionoya, M.; Kimura, E.; Espinosa, E.; Barbe, J.-M.; Guilard, R. Synthesis and Crystal Structures of Palladium(II) Complexes of 1,11-Bis(2-Pyridylmethyl)-1,4,8,11-Tetraazacyclotetradecane-5,7-Dione. *J. Chem. Soc., Dalton Trans.* **2001**, No. 6, 898–901. https://doi.org/10.1039/B009208H.

(34) Hay, R. W.; Pujari, M. P.; Perotti, A. Copper(II) and Nickel(II) Complexes of Mono-Oxocyclam(5-Oxo-1,4,8,11-Tetraazacyclotetradecane). Synthetic and Potentiometric Studies. *Transit. Met. Chem.* **1985**, *10* (10), 396–399. https://doi.org/10.1007/BF00618853.

(35) Riche, F.; Pasqualini, R.; Duatti, A.; Vidal, M. Etude de La Complexation Du Coeur [$^{99m}TcO_2^+$] Par Le 2,4-Dioxo-1,5,8,12-Tétraazacyclotétradécane, Le 2-Oxo-1,5,8,12-Tétraazacyclotétradécance, et Leurs Dérivés Méthylés En Position 3. *Int. J. Rad. Appl. Instr. A.* **1992**, *43* (3), 437–442. https://doi.org/10.1016/0883-2889(92)90118-X.

(36) Camus, N.; Halime, Z.; Le Bris, N.; Bernard, H.; Platas-Iglesias, C.; Tripier, R. Full Control of the Regiospecific *N*-

Functionalization of *C*-Functionalized Cyclam Bisaminal Derivatives and Application to the Synthesis of Their TETA, TE2A, and CB-TE2A Analogues. *J. Org. Chem.* **2014**, *79* (5), 1885–1899. https://doi.org/10.1021/jo4028566.

(37) Le Bihan, T.; Navarro, A.-S.; Le Bris, N.; Le Saëc, P.; Gouard, S.; Haddad, F.; Gestin, J.-F.; Chérel, M.; Faivre-Chauvet, A.; Tripier, R. Synthesis of *C*-Functionalized TE1PA and Comparison with Its Analogues. An Example of Bioconjugation on 9E7.4 mAb for Multiple Myeloma ^{64}Cu-PET Imaging. *Org. Biomol. Chem.* **2018**, *16* (23), 4261–4271. https://doi.org/10.1039/C8OB00499D.

(38) Tripier, R.; Camus, N. Procédés de Préparation de Composés Tétraazacycloalcanes Fonctionnels à l'aide d'un Composé Cyclique Bisaminal Particulier. WO2013072491A1, 2013. https://patents.google.com/patent/WO2013072491A1/fr (accessed 2022-03-28).

(39) Hay, R. W.; Pujari, M. P.; Moodie, W. T.; Craig, S.; Richens, D. T.; Perotti, A.; Ungaretti, L. Synthetic and Equilibrium Studies on Copper(II), Nickel(II), and Palladium(II) Complexes of *N,N′,N″,N‴*-Tetrakis(2-Hydroxyethyl)-1,4,8,11-Tetra-Azacyclotetradecane (L); Kinetics of the Acid Dissociation of the Copper(II) Complex and X-Ray Structural Characterisation of the Nickel(II) Complex $[NiLH^{-1}][ClO_4]$. *J. Chem. Soc., Dalton Trans.* **1987**, No. 11, 2605–2613. https://doi.org/10.1039/DT9870002605.

(40) Delgado, R.; Da Silva, J. J. R. F.; Amorim, M. T. S.; Cabral, M. F.; Chaves, S.; Costa, J. Dissociation Constants of BrØnsted Acids in D_2O and H_2O: Studies on Polyaza and Polyoxa-Polyaza Macrocycles and a General Correlation. *Anal. Chim. Acta.* **1991**, *245*, 271–282. https://doi.org/10.1016/S0003-2670(00)80232-9.

(41) Chandrasekhar, S.; Waltz, W. L.; Quail, J. W.; Prasad, L. Structural Studies and Redox Reactivity of Platinum Complexes of 14-Membered Tetraaza Macrocyclic Ligands. *Can. J. Chem.* **1997**, *75* (10), 1363–1374. https://doi.org/10.1139/v97-164.

(42) Rasmussen, L.; Jørgensen, K. Palladium (II) Complexes I. Spectra and Formation Constants of Ammonia and Ethylenediamine Complexes. *Acta Chem. Scand.* **1968**, *22*, 2313–2323.

(43) Vanquickenborne, L. G.; Ceulemans, A. Ligand Field Spectra of Square-Planar Platinum(II) and Palladium(II) Complexes. *Inorg. Chem.* **1981**, *20* (3), 796–800. https://doi.org/10.1021/ic50217a033.

(44) Anderegg, G. The Stability of the Palladium(II) Complexes with Ethylenediamine, Diethylenetriamine and Tris(β-Aminoethyl)-Amine. *Inorg. Chim. Acta.* **1986**, *111* (1), 25–30. https://doi.org/10.1016/S0020-1693(00)82211-2.

(45) Blake, A. J.; Gould, R. O.; Hyde, T. I.; Schröder, M. Stabilisation of Monovalent Palladium by Tetra-Aza Macrocycles. *J. Chem. Soc., Chem. Commun.* **1987**, *0* (6), 431–433. https://doi.org/10.1039/C39870000431.

(46) Blake, A. J.; Hyde, T. I.; Schroder, M. Tetrahedral Distortion in Palladium(II) Macrocyclic Complexes: The Single Crystal X-Ray Structure of $[Pd(Tbc)](PF_6)_2$ = 0.4 $MeNO_2$ (Tbc = 1,4,8,11-Tetrabenzyl-1,4,8,11-Tetra-Azacyclotetradecane). *J. Chem. Soc., Chem. Commun.* **1987**, No. 22, 1730–1732. https://doi.org/10.1039/C39870001730.

(47) Tušek-Božić, L.; Matijašić, I.; Bocelli, G.; Sgarabotto, P.; Furlani, A.; Scarcia, V.; Papaioannou, A. Preparation, Characterization and Activity of Palladium(II) Halide Complexes with Diethyl 8-Quinolylmethylphosphonate (8-Dqmp). X-Ray Crystal Structure of $[8\text{-}dqmpH]_2[PdCl_4]\cdot 2H_2O$ and [8- Inorg. Chim. Acta. $dqmpH]_2[Pd_2Br_6]$. *Inorg. Chim. Acta.* **1991**, *185* (2), 229–237. https://doi.org/10.1016/S0020-1693(00)85448-1.

(48) Kumar, S.; Jha, R. R.; Yadav, S.; Gupta, R. Pd(II) Complexes with Amide-Based Macrocycles: Syntheses, Properties and Applications in Cross-Coupling Reactions. *New J. Chem.* **2015**, *39* (3), 2042–2051. https://doi.org/10.1039/C4NJ01300J.

(49) Liang, X.; Sadler, P. J. Cyclam Complexes and Their Applications in Medicine. *Chem. Soc. Rev.* **2004**, *33* (4), 246–266. https://doi.org/10.1039/B313659K.

(50) Jaiswal, Y.; Kumar, Y.; Kumar, A. The Palladium(II)-Catalyzed Regioselective *Ortho*-C–H Bromination/Iodination of Arylacetamides with *in Situ* Generated Imidic Acid as the Directing Group: Mechanistic Exploration. *Org. Biomol. Chem.* **2019**, *17* (28), 6809–6820. https://doi.org/10.1039/C9OB01082C.

(51) Liang, X.; Weishäupl, M.; Parkinson, J. A.; Parsons, S.; McGregor, P. A.; Sadler, P. J. Selective Recognition of Configurational Substates of Zinc Cyclam by Carboxylates: Implications for the Design and Mechanism of Action of Anti-HIV Agents. *Chem. Eur. J.* **2003**, *9* (19), 4709–4717. https://doi.org/10.1002/chem.200304808.

(52) Roger, M.; Lima, L. M. P.; Frindel, M.; Platas-Iglesias, C.; Gestin, J.-F.; Delgado, R.; Patinec, V.; Tripier, R. Monopicolinate-Dipicolyl Derivative of Triazacyclononane for Stable Complexation of Cu^{2+} and $^{64}Cu^{2+}$. *Inorg. Chem.* **2013**, *52* (9), 5246–5259. https://doi.org/10.1021/ic400174r.

(53) Gans, P.; Sabatini, A.; Vacca, A. Investigation of Equilibria in Solution. Determination of Equilibrium Constants with the HYPERQUAD Suite of Programs. *Talanta* **1996**, *43* (10), 1739–1753. https://doi.org/10.1016/0039-9140(96)01958-3.

(54) Sweeton, F. H.; Mesmer, R. E.; Baes, C. F. Acidity Measurements at Elevated Temperatures. VII. Dissociation of Water. *J. Solution Chem.* **1974**, *3* (3), 191–214. https://doi.org/10.1007/BF00645633.

(55) Elding, L. I. Palladium(II) Halide Complexes. I. Stabilities and Spectra of Palladium(II) Chloro and Bromo Aqua Complexes. *Inorg. Chim. Acta.* **1972**, *6*, 647–651. https://doi.org/10.1016/S0020-1693(00)91874-7.

(56) Chai, J.-D.; Head-Gordon, M. Long-Range Corrected Hybrid Density Functionals with Damped Atom–Atom Dispersion Corrections. *Phys. Chem. Chem. Phys.* **2008**, *10* (44), 6615–6620. https://doi.org/10.1039/B810189B.

(57) Chai, J.-D.; Head-Gordon, M. Systematic Optimization of Long-Range Corrected Hybrid Density Functionals. *J. Chem. Phys.* **2008**, *128* (8), 084106. https://doi.org/10.1063/1.2834918.

(58) Frisch, M. J.; Trucks, G. W.; Schlegel, H. B.; Scuseria, G. E.; Robb, M. A.; Cheeseman, J. R.; Scalmani, G.; Barone, V.; Petersson, G. A.; Nakatsuji, H.; Li, X.; Caricato, M.; Marenich, A. V.; Bloino, J.; Janesko, B. G.; Gomperts, R.; Mennucci, B.; Hratchian, H. P.; Ortiz, J. V.; Izmaylov, A. F.; Sonnenberg, J. L.; Williams-Young, D.; Ding, F.; Lipparini, F.; Egidi, F.; Goings, J.; Peng, B.; Petrone, A.; Henderson, T.; Ranasinghe, D.; Zakrzewski, V. G.; Gao, J.; Rega, N.; Zheng, G.; Liang, W.; Hada, M.; Ehara, M.; Toyota, K.; Fukuda, R.; Hasegawa, J.; Ishida, M.; Nakajima, T.; Honda, Y.; Kitao, O.; Nakai, H.; Vreven, T.; Throssell, K.; Montgomery, J. A., Jr.; Peralta, J. E.; Ogliaro, F.; Bearpark, M. J.; Heyd, J. J.; Brothers, E. N.; Kudin, K. N.; Staroverov, V. N.; Keith, T. A.; Kobayashi, R.; Normand, J.; Raghavachari, K.; Rendell, A. P.; Burant, J. C.; Iyengar, S. S.; Tomasi, J.; Cossi, M.; Millam, J. M.; Klene, M.; Adamo, C.; Cammi, R.; Ochterski, J. W.; Martin, R. L.; Morokuma, K.; Farkas, O.; Foresman, J. B.; Fox, D. J. Gaussian. Gaussian 16, Revision B.01, 2016.

(59) Peterson, K. A.; Figgen, D.; Dolg, M.; Stoll, H. Energy-Consistent Relativistic Pseudopotentials and Correlation Consistent Basis Sets for the 4d Elements Y–Pd. *J. Chem. Phys.* **2007**, *126* (12), 124101. https://doi.org/10.1063/1.2647019.

(60) Weigend, F.; Ahlrichs, R. Balanced Basis Sets of Split Valence, Triple Zeta Valence and Quadruple Zeta Valence

Quality for H to Rn: Design and Assessment of Accuracy. *Phys. Chem. Chem. Phys.* **2005**, *7* (18), 3297–3305. https://doi.org/10.1039/B508541A.
(61) Cancès, E.; Mennucci, B.; Tomasi, J. A New Integral Equation Formalism for the Polarizable Continuum Model: Theoretical Background and Applications to Isotropic and Anisotropic Dielectrics. *J. Chem. Phys.* **1997**, *107* (8), 3032–3041. https://doi.org/10.1063/1.474659.
(62) Tomasi, J.; Mennucci, B.; Cammi, R. Quantum Mechanical Continuum Solvation Models. *Chem. Rev.* **2005**, *105* (8), 2999–3094. https://doi.org/10.1021/cr9904009.
(63) Sheldrick, G. M. SHELXT – Integrated Space-Group and Crystal-Structure Determination. *Acta. Cryst. A.* **2015**, *71* (1), 3–8. https://doi.org/10.1107/S2053273314026370.
(64) Sheldrick, G. M. Crystal Structure Refinement with SHELXL. *Acta. Cryst. C.* **2015**, *71* (1), 3–8. https://doi.org/10.1107/S2053229614024218.

SYNOPSIS TOC.

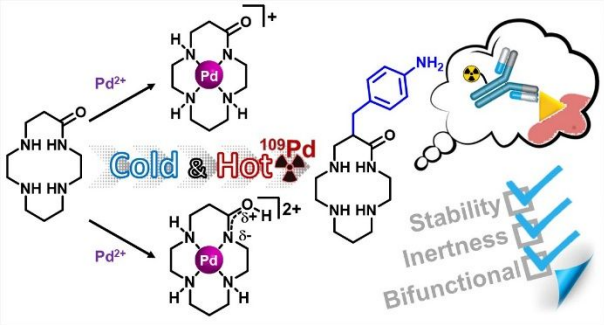

We provide a comprehensive study on the coordination of oxocyclam with Pd(II), including the synthesis of a novel bifunctional analogue and detailed characterization of the resulting complexes using various techniques, revealing diverse configurations and highlighting oxocyclam's potential as a chelating agent for palladium-based applications, including radiolabeling.